Electron-phonon interaction in $La_{2-x}Sr_xCuO_4$ investigated by Raman scattering

Shigeki Nimori* and Shigenobu Sakita
Venture Business Laboratory, Hiroshima University, Kagamiyama 2-313, Higashi-Hiroshima 739-8527, Japan

Fumihiko Nakamura and Toshizo Fujita
Department of Quantum Matter, ADSM, Hiroshima University, Higashi-Hiroshima 739-8526, Japan

Hiroaki Hata, Norio Ogita, and Masayuki Udagawa
Faculty of Integrated Arts and Sciences, Hiroshima University Kagamiyama 1-7-1, Higashi-Hiroshima 739-8521, Japan
(Received 6 December 1999)

Using high-quality single crystals of $La_{2-x}Sr_xCuO_4$, Raman scattering spectra in the (c,c) geometry have been investigated in different Sr concentrations ($x=0,0.1,0.113,0,15,0.22$) and in the wide temperature region. It has been found that the apical oxygen vibration along the c axis shows the following anomalous behaviors in the dependences of the Sr concentration and temperature. With the increase of the Sr concentration, the peak intensity abruptly decreases from $x=0$ to 0.1 and its line shape becomes asymmetric. In the temperature dependence, its energy is almost constant or slightly decreases with decreasing temperature, and also its intensity decreases above 100 K universally in the doped samples. In addition, the background intensities increase with increasing x, except for $x=0.113$ at 6 K, where ''1/8 problem'' occurs. This increase shows that the background response is caused by an electronic excitation because the magnetic one is forbidden in the (c,c) spectra. The decrease of the background at $x=0.113$ at 6 K is understood by the formation of charge density wave. The asymmetric line shapes of the apical oxygen vibration are well explained by the Fano model, which is based on the interference effect between the phonon and electronic excitations. Furthermore, the abrupt decrease of the intensity from $x=0$ to 0.1 is also explained by the introduction of the electron-phonon interaction. The correlation between the obtained electron-phonon interaction and T_c has been found in the Sr-concentration dependence.

I. INTRODUCTION

Concerning the formation of a Cooper pair in conventional superconductors, the electron-phonon coupling plays an important role. In the high-T_c cuprates, on the other hand, it is usually accepted that a mechanism different from conventional superconductors generates the electron pairs, for example, the magnetic interaction model. It is also considered that the electron-phonon interaction makes few contributions to superconductivity in the high-T_c cuprates. However, it is not revealed that the electron-phonon interaction gives no contribution to superconductivity.

In an early stage, extensive investigations were performed in terms of the electron-phonon interaction. For $La_{2-x}Sr_xCuO_4$ (LSCO), the isotope effect was observed,[1–3] but the results were too complicated to reach a conclusion about the contribution of the electron-phonon interaction. Despite the huge efforts to reveal the collaboration effect of spin and lattice, we think that superconductivity in the high-T_c cuprates is not understood well. Therefore, we should have a new understanding about the electron-phonon interaction.

Among the high-T_c cuprates, the La_2CuO_4-based system has a simple crystal structure because of a single CuO_2 layer. In addition, high-quality single crystals can be obtained in the wide carrier-concentration region. Thus, this crystal is a suitable system for a systematic investigation of the different carrier concentrations.

Up to this time, many Raman scattering studies have been carried out in the oxide superconductors, and the correlation between phonon and electrons states has been discussed, especially in Y-Ba-Cu-O (YBCO) systems.[4–6] To our knowledge, however, there is no Raman scattering study focused on the electron-phonon interaction in the wide carrier range for LSCO. From theoretical calculations, Krakauer *et al.* have reported that the apical oxygen vibration along the c axis has a large electron-phonon interaction for $La_{1.85}Sr_{0.15}CuO_4$.[7] Thus a systematic Raman scattering study is necessary for LSCO with the different Sr concentrations (x) in order to clarify the correlation between phonon and electron states.

LSCO shows a structural phase transition from the tetragonal phase (THT) of $I4/mmm$ to the orthorhombic one (OMT) of *Bmab* with decreasing temperature. The structural phase transition temperature (T_d) descends with increasing x. From a group theoretical analysis, the number of the totally symmetric Raman-active phonons for each structure is estimated as $N_R(\mathrm{THT})=2A_{1g}$ and $N_R(\mathrm{OMT})=5A_g$. Phonons with total symmetry of A_{1g} or A_g appear in the polarization spectra of (a,a), (b,b), and (c,c). The symbol (x,y) denotes the polarization condition, where x and y are the polarization directions of the incident and scattered light, respectively. Since two-magnon excitations are excluded from the selection rule in the (c,c) geometry, the (c,c) spectrum is suitable to study the electron-phonon interaction. We have mainly studied symmetry-allowed phonons for the tetragonal phase, where two vibrations along the c axis are Raman active: One is the in-phase motion between La and apical oxygen at $\sim 230\ \mathrm{cm}^{-1}$ (P_1) and the other is the apical oxy-

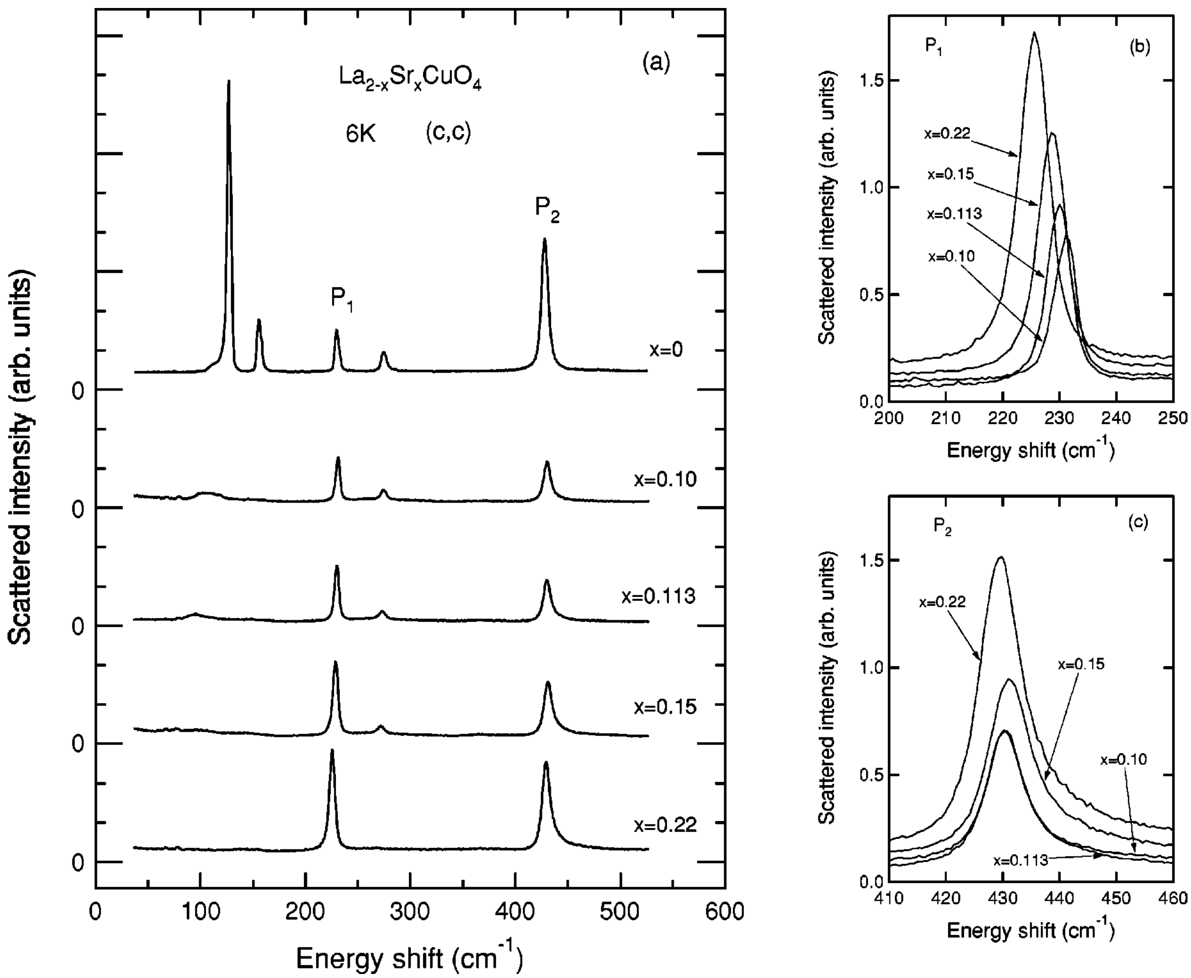

FIG. 1. (a) Sr-concentration dependence of the (*c*,*c*) Raman spectra in $La_{2-x}Sr_xCuO_4$ at 6 K. Each spectrum is shifted vertically to avoid the overlaps. (b) Enlarged Raman spectra around P_1. (c) Enlarged Raman spectra around P_2.

gen vibration at $\sim$440 cm^{-1} (P_2).

In this paper a systematic study of (*c*,*c*) Raman spectra has been carried out in the wide carrier range ($x=0-0.22$) and the wide temperature region. In Sec. II we describe the preparation of the single-crystal and Raman scattering measurements. In Sec. III, the experimental results of the temperature and Sr-concentration dependence of (*c*,*c*) Raman spectra are presented. A discussion based on the electron-phonon interaction model is also presented.

II. EXPERIMENT

$La_{2-x}Sr_xCuO_4$ ($x=0$,0.1,0.113,0.15,0.22) single crystals were grown by a traveling-solvent floating-zone method. After the surface polish, the samples were annealed in a flowing O_2 atmosphere at 920 °C for 50 h and 500 °C for 50 h to minimize the strains and to obtain the oxygen stoichiometric specimens.

In the Raman scattering measurements, a 514.5-nm light of an Ar^+ laser with an output power of 15 mW was employed as the incident beam. The nearly backward scattered light was analyzed by a triple monochromator (JASCO, NR-1800), and the analyzed light was detected by a charge-coupled device (CCD) multichannel detector (Princeton Instruments). For the measurements below room temperature, the sample was put in the flow-type cryostat using liquid ^{4}He and the sample space was filled with a ^{4}He heat exchange gas to cool the sample and to avoid local heating of the sample by the incident beam.

III. RESULTS AND DISCUSSION

The Sr-concentration dependence of the (*c*,*c*) Raman spectra at 6 K is shown in Fig. 1, where (a) is the spectra in the energy region between 0 and 600 cm^{-1} and (b) and (c) are the detailed spectra in the vicinity of P_1 and P_2, respectively. In Fig. 1(a), each spectrum is shifted vertically to avoid overlaps. Two obvious phonons have been observed for $x=0.22$ and five phonons for the other crystals. Since the crystal with $x=0.22$ belongs to the THT phase and others to the OMT phase at 6 K, the observed number of phonons agrees with the expected one from the group theoretical analysis. The peaks marked by P_1 and P_2 correspond to the in-phase vibration between La/Sr and apical oxygen and the apical oxygen vibration along the *c* axis, respectively. The other three peaks, except for $x=0.22$, are the symmetry-allowed phonons in the OMT phase and their intensities decrease with the increase of *x*. The present result for $x=0.22$ clearly shows that superconductivity appears even in the tetragonal phase, since the crystal has $T_c=28.5$ K.

The Sr-concentration dependence of the peak energy for

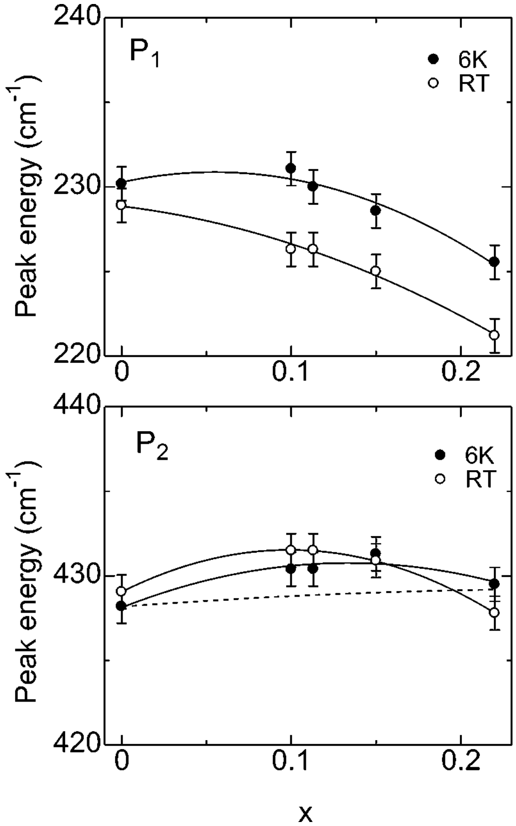

FIG. 2. Concentration dependence of the energy of P_1 and P_2 at room temperature and 6 K. Solid lines are a guide to the eyes. The dashed line indicates the estimated energy for P_2 from the Fano analysis.

P_1 and P_2 at 6 K and room temperature is shown in Fig. 2, where the error bars denote the determination accuracy of the peak energy within ± 1 cm^{-1} and the solid lines are drawn to guide the eye. The energy of P_1 decreases almost monotonically with increasing x at 6 K and room temperature, while that of P_2 increases once and then decreases for both temperatures. A similar decrease of the energy for P_1 has been also observed in the $La_{2-x}Sr_xNiO_4$ (LSNO) system and has been explained by the decrease of the ionic interaction in the La-O layers by the carrier doping.[8] The same mechanism occurs also in the LSCO system. However, the upturn dependence for P_2 is not the case, since the energy of P_2 in LSNO is almost constant in the concentration region less than 0.3. Later we describe the details of the analysis using the Fano model. Here, for comparison, the result estimated by the model for P_2 is shown by the dashed line in Fig. 2. The electron-phonon interaction does not reproduce the concentration dependence of the energy of P_2. Thus the additional ionic interaction due to the carrier doping is important for P_2 in LSCO. Since such interaction is not derived separately from our experiments, a normal-mode calculation based on a first-principles calculation is necessary in order to understand the present result.

As shown in Fig. 2, the energy of P_1 increases with decreasing temperature for all concentrations. This is the ordinary behavior of phonons, since the bond length decreases with a decrease of temperature. However, for P_2 in $x \leqslant 0.15$, its energy is almost constant or slightly decreases with decreasing temperature. Furthermore, such anomalous temperature dependence changes to an ordinary one in the concentration region larger than 0.15, which is called the overdoped region.

The concentration dependence of the intensities of P_1 and P_2 is different, as shown in Fig. 1(a). The intensity of P_2 dramatically decreases from $x=0$ to 0.1 and gradually increases for $x \geqslant 0.1$, while that of P_1 increases monotonically. The increasing rate of P_1 and P_2 is almost similar for $x \geqslant 0.1$, as shown in Figs. 1(b) and 1(c). Generally, the intensity of the phonon is proportional to the displacement of the ions. Thus the intensity of P_2 is expected to be larger than that of P_1, since the displacement of the apical oxygen vibration is larger by about three times than that of La/Sr of P_1, according to our previous calculation using the GF-matrix method.[9] This relationship, in fact, is held for $x=0$ and Sr_2RuO_4.[10] The abrupt suppression of P_2 was once explained by the shielding effect by doped carriers in our previous report on $La_2CuO_{4+\delta}$.[9] However, the present result suggests that the shielding effect is not the origin of the intensity change, because the increasing rate of the intensity for P_1 and P_2 is similar from $x=0.1$ to 0.22. According to the Fano effect, the peak intensity depends on the electron-phonon coupling. For $x=0$, the intensity of the uncoupled phonon is large because of $V=0$, where V is an interaction parameter. Thus the abrupt decrease of P_2 is explained by the introduction of the electron-phonon interaction for $x \geqslant 0.1$ and the concentration dependence is qualitatively explained by the change of the electron-phonon interaction parameter V, which is shown in Fig. 8, below. For P_1, a similar mechanism cannot be simply applied, because the line shape is not so asymmetric in the (c,c) spectra. However, we note that P_1 is anomalous in the (a,a) spectra, where the intensity of P_1 is much weaker than that of P_2 and its energy decreases by 10 cm^{-1} for $x=0$. A detailed report on P_1 will appear in our next paper.

As the representative temperature dependence of the (c,c) Raman spectra, the result for $x=0.22$ is shown in Fig. 3. Each spectrum is shifted vertically to avoid overlaps of the spectrum. The intensities of P_1 and P_2 slightly decrease below T_c. However, the clear suppression at T_c has not been observed for other doped samples. Thus, to obtain the final conclusion experimentally, we need further precise measurements using different samples.

To understand the temperature dependence of the intensities of P_2, we employed the integrated intensity ratio of $I(P_2)/I(P_1)$. The intensity of P_1 is taken as the reference for that of P_2 to exclude the change due to experimental conditions. Figure 4 shows the temperature dependence of the integrated-intensity ratio of $I(P_2)/I(P_1)$ in a log-log diagram, where the ratio of each Sr concentration is normalized to unity at the lowest temperature. In the estimation of the integrated intensities, the backgrounds were eliminated. The dashed line denotes the ratio estimated by the Bose factor. The Raman scattering intensity on the Stokes side is proportional to $n+1$, where n represents the Bose factor. For Sr_2RuO_4, which is the same layered perovskite structure as LSCO, $I(P_2)/I(P_1)$ is well explained by the Bose factor correction.[9] The temperature dependence obtained of

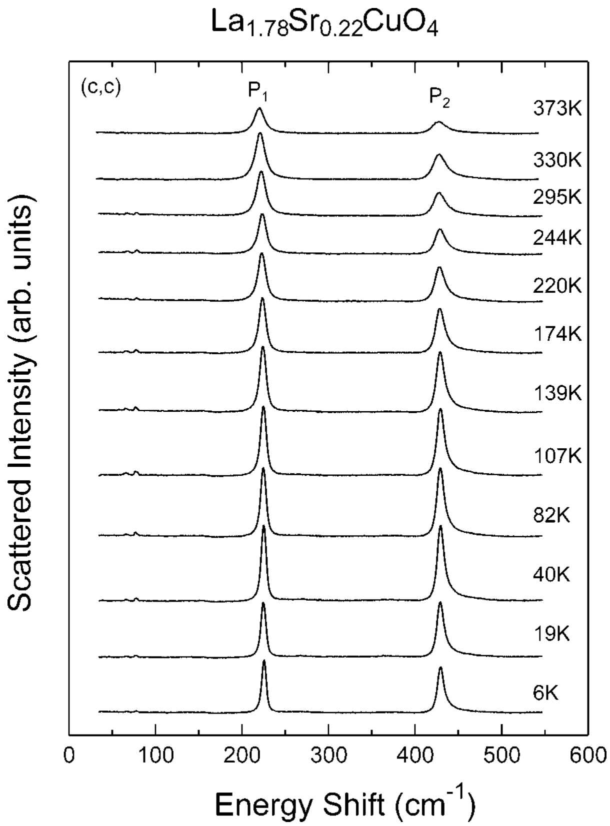

FIG. 3. Temperature variation of the (c,c) Raman spectra in $La_{1.78}Sr_{0.22}CuO_4$. Each spectrum is shifted vertically to avoid overlaps.

$I(P_2)/I(P_1)$ for doped LSCO is not explained by the simple Bose factor correction.

Our previous report suggested that the temperature dependence of the integrated-intensity ratio for $x=0.15$ might be caused by charge confinement.[9] However, since the suppression of $I(P_2)/I(P_1)$ above 100 K is universal for doped samples, a clear correlation between the charge confinement and $I(P_2)/I(P_1)$ has not been observed. Therefore, for the suppression of $I(P_2)/I(P_1)$ above 100 K, a different consideration is necessary. The linewidth of P_2 at 6 K is twice as much as that of P_1, which is close to the instrumental limit. This fact implies that the apical oxygen vibration is not fully coherent due to spatial disorder or randomness. Furthermore, the temperature dependence of the linewidth of P_2 is well explained by that of the Debye-Waller factor for apical oxygen measured by Braden *et al.*[11] These results denote that the disorder of the apical oxygen increases at higher temperature. As related experimental evidence of the spatial disorder of the oxygen, we point out that the phonon of the excess oxygen disappears above 220 K in $La_2CuO_{4+\delta}$.[9] That experimental facts suggest that the oxygen does not stay at a certain position above 220 K. The suppression for the P_2 intensity in LSCO reminds us of a similar mechanism due to randomness or disorder.

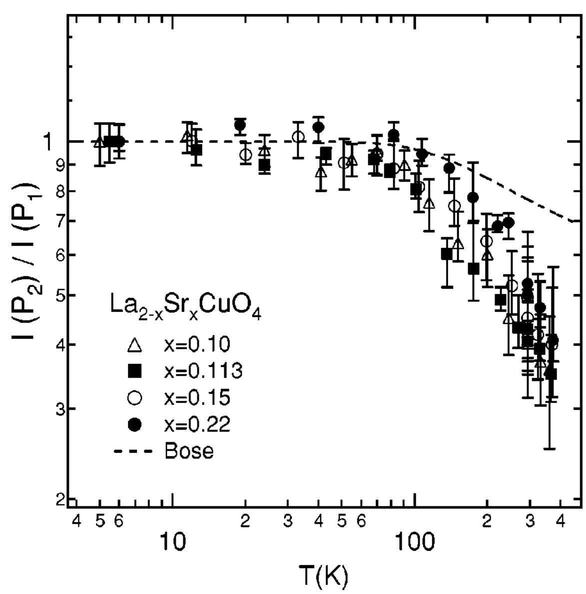

FIG. 4. Temperature dependence of the energy-integrated Raman scattered intensity of $I(P_2)/I(P_1)$ in a log-log plot for $La_{2-x}Sr_xCuO_4$. Each ratio is scaled at the lowest temperature. The dashed line indicates the result estimated by the Bose factor.

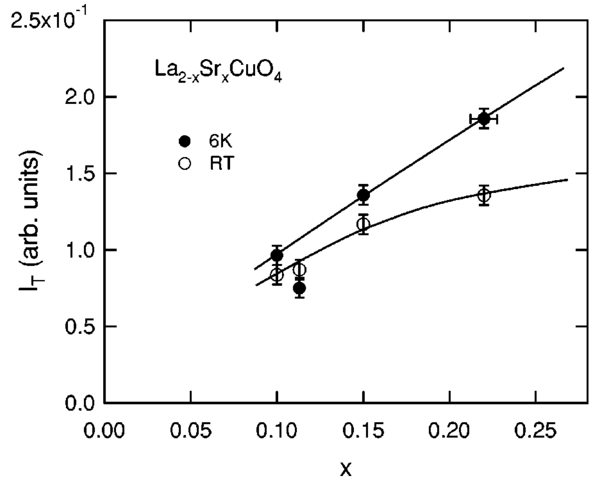

FIG. 5. x dependence of the total background intensity (I_T) at 6 K and room temperature. The error bar for the horizontal direction at $x=0.22$ is caused by a deviation from the stoichiometric oxygen concentration.

Next, we discuss the experimental results for the broad background intensity. As shown in Fig. 1, the broad background intensity apparently exhibits a carrier dependence. The broad responses correspond to an electronic excitation in principle, since the magnetic excitation is forbidden in the (c, c) spectra by the symmetry selection rule for two-magnon excitations. Figure 5 shows the concentration dependence of the total background intensity (I_T) at 300 and 6 K. At 300 K, the intensity increases monotonically with increasing x, while that at 6 K is proportional to x except for $x=0.113$, where the superconducting temperature (T_c) is suppressed and this phenomenon is known as the ''1/8 problem'' in the La-cuprate system. The proportional increase of the background intensity to x concludes that the origin of the broad response in the (c,c) spectra is electronic.

By carrier doping, the line shape of P_2 becomes asymmetric as shown in Fig. 1. These asymmetrical line shapes are not explained by a multimode analysis. In order to explain the asymmetric line shapes of P_2, we have employed the interference model formulated by Fano.[12,13] This model takes into account the interference between a sharp excitation

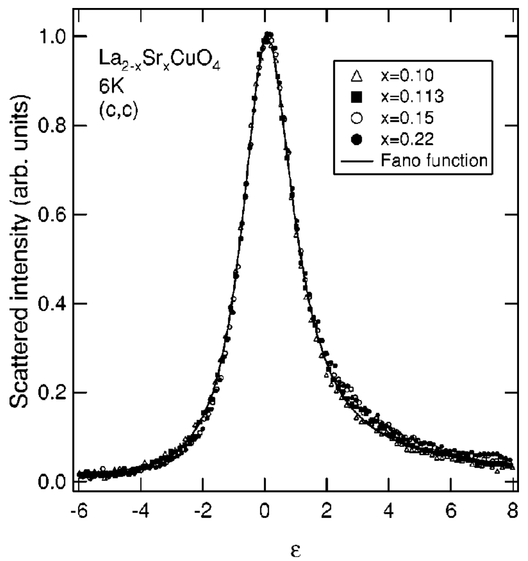

FIG. 6. Line shapes of the P_2 are plotted in reduced units ε for various Sr concentrations at 6 K. The amplitudes are normalized by $(S-I_{BG})/I_F q^2$. The solid line is a representative fitting by the Fano function.

and broad response. In order to fit the experimental results, we use the following line shape function of S:

$$S=\pi\rho T_e^2\frac{(q+\varepsilon)^2}{1+\varepsilon^2}+I_{BG}, \quad (1)$$

where q, ε, and Γ are expressed as $q=T_p/\pi\rho V T_e$, $\varepsilon=(\omega-\omega_p)/\Gamma$, and $\Gamma=\pi\rho V^2$. Here ρ denotes the state density of the electronic excitation, ω_p and V the uncoupled phonon energy and electron-phonon interaction, and T_p and T_e the transition probabilities of the phonon and electronic excitation, respectively. I_{BG} means the background intensity, which is not directly related to the Fano effect. From the fittings to the experimental line shapes using Eq. (1), one set of parameters of q, Γ, ω_p, $\pi\rho T_e^2$ $(=I_F)$, and I_{BG} is derived.

The representative fitted line shape at 6 K is shown in Fig. 6, where the vertical axis is the normalized value by the formula of $(S-I_{BG})/I_F q^2$ and the horizontal one is ε. The line shapes of P_2 are well explained by the Fano model as shown in Fig. 6. The reduced $(S-I_{BG})/I_F q^2$ seems to fall onto the universal curve. However, a systematic change depending on x has been obtained. With increasing x, the intensity at the lower-energy side of the peak decreases and that at the higher-energy one increases. The Fano shapes in LSCO are different from other oxide superconductors, since the dips exist on the low-energy sides for LSCO, but that on the higher-energy side for YBCO. This difference corresponds to the sign of the asymmetric parameter q. In the case of LSCO, the asymmetric parameter q is positive, while q is less than 0 in YBCO.[4,5] Above and below T_c, this remarkable change has not been observed for the line shape of P_2. We note that the value of ρT_e of LSCO is rather smaller than that of other high-T_c cuprates. This is related to the lower conductivity of LSCO than that of YBCO.

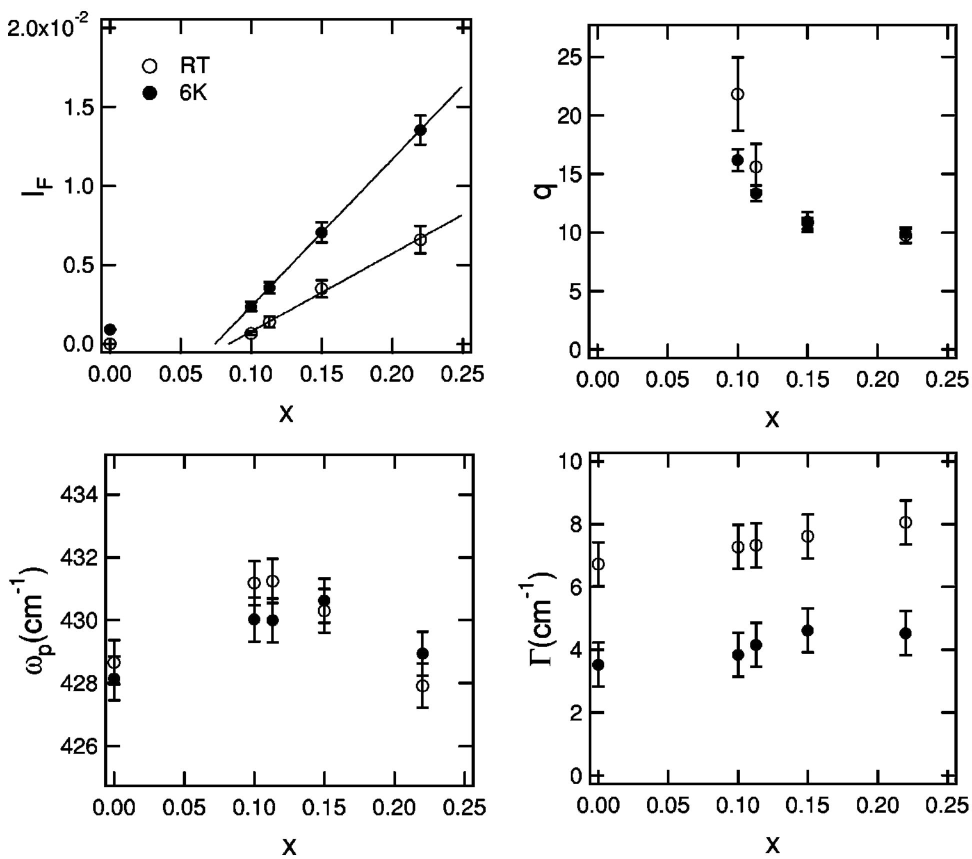

FIG. 7. Sr-concentration dependence of the Fano parameters I_F, q, ω_p, and Γ at 6 K and room temperature. Solid lines in I_F vs x are guides to the eyes.

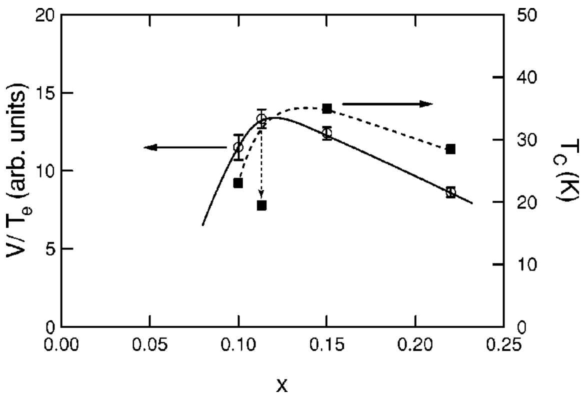

FIG. 8. Sr-concentration dependence of V/T_e and T_c at 6 K. Solid and dashed lines are the guide to the eyes. The suppression of T_c at $x=0.113$ is shown by the dot-dashed line.

The x dependences of the q, Γ, ω_p, and I_F obtained for 6 K and room temperature are shown in Fig. 7, where I_F is the background related to the Fano contribution. The electronic contribution ρT_e increases with increasing x, since the asymmetric parameter q decreases. I_F increases proportionally with increasing x, and the extrapolated carrier concentration at $I_F=0$ is very close to the lowest concentration where superconductivity appears. This agreement suggests a correlation between the electron-phonon interaction for P_2 and superconductivity.

From each set of fitted parameters, V/T_e can be calculated by using the equation $V/T_e=\sqrt{\Gamma/I_F}$. The concentration dependence of V/T_e and T_c is shown in Fig. 8. We regard that T_e is independent of x in the same Raman scattering geometry, since T_e is the transition probability of the electronic excitation. Thus the concentration dependence of V/T_e corresponds to that of V. The present results show the correlation between the electron-phonon interaction and T_c; however, it is not clear whether the present electron-phonon interaction is the primary contribution to the pairing mechanism or not.

We mention the low proportion of I_F to the total background intensity (I_T) in Fig. 5. This implies that only a small percentage of the electronic response originates in the Fano effect. The intensity of the electronic excitation in the Raman spectra is the integrated value by wave vector for the whole Brillouin zone, while P_2 is the excitation at the Brillouin zone center. Therefore, the present result shows that the fraction of electronic excitation at zone center is rather small. We comment on the decrease of the total background intensity (I_T) of $x=0.113$ at 6 K. This decrease corresponds to the reduction in the state density of the electronic excitation in the whole Brillouin zone, since I_F does not show an anomalous decrease at $x=0.113$ as shown in Fig. 7. We believe that the present result of I_T is experimental evidence of the formation of a charge-ordered state at $x=0.113$.

Finally, we summarize the present results and the remaining problems. As described above, the apical oxygen vibration in the (c,c) spectra shows many anomalous behaviors. Among them, the abrupt intensity decrease from $x=0$ to 0.1 and the asymmetric line shape are well explained by the Fano interference model. Furthermore, the obtained electron-phonon interaction correlates with T_c in the concentration dependence. Recently, a neutron scattering study has reported the importance of the electron-phonon coupling for $La_{1.85}Sr_{0.15}CuO_4$.[14] However, the quantitative contribution of the electron-phonon interaction to the pairing mechanism remains unclear. In order to draw a final conclusion about the mechanism, a theoretical calculation in terms of the phonon side will be necessary. As other anomalous properties of P_2, the concentration and temperature dependence of the energy of P_2 is pointed out. To understand this, we emphasize again that a precise normal-mode calculation based on a first-principles calculation is necessary.

ACKNOWLEDGMENTS

This work is supported by a Grant-in-Aid for Scientific Research, Japanese Ministry of Education, Science and Culture. The Raman scattering experiment was also supported by the cryogenic center of Hiroshima University.

*Present address: Tsukuba Magnet Laboratory, National Research Institute for Metals, Tsukuba, Ibaraki 305-0003, Japan.

[1] M. K. Crawford, W. E. Farneth, E. M. McCarron III, R. L. Harlow, and A. H. Moudden, Science **250**, 1390 (1990).

[2] M. K. Crawford, M. N. Kunchur, W. E. Farneth, E. M. McCarron III, and S. J. Poon, Phys. Rev. B **41**, 282 (1990).

[3] Guo-meng Zhao, K. K. Singh, A. P. B. Sinha, and D. E. Morris, Phys. Rev. B **52**, 6840 (1995).

[4] S. L. Cooper, M. V. Klein, B. G. Pazol, J. P. Rice, and D. M. Ginsberg, Phys. Rev. B **37**, 5920 (1988).

[5] E. T. Heyen, M. Cardona, J. Karpinski, E. Kaldis, and S. Rusiecki, Phys. Rev. B **43**, 12 958 (1991).

[6] C. Thomsen, M. Cardona, R. Liu, T. Ruf, B. Gegenheimer, and E. T. Heyen, Physica C **162-164**, 1079 (1989).

[7] H. Krakauer, W. E. Pickett, and R. E. Cohen, Phys. Rev. B **47**, 1002 (1993).

[8] M. Udagawa, T. Yamaguchi, Y. Nagaoka, N. Ogita, M. Kato, Y. Maeno, T. Fujita, and K. Ohbayashi, Phys. Rev. B **47**, 11 391 (1993).

[9] M. Udagawa, H. Hata, S. Nimori, T. Minami, N. Ogita, S. Sakita, F. Nakamura, T. Fujita, and Y. Maeno, J. Phys. Soc. Jpn. **67**, 2529 (1998).

[10] S. Nimori, S. Sakita, N. Ogita, Z. Q. Mao, Y. Maeno, and M. Udagawa, Physica B **281&282**, 961 (2000).

[11] M. Braden, P. Schweiss, G. Heger, W. Reichardt, Z. Fisk, K. Gamayunov, I. Tanaka, and H. Kojima, Physica C **223**, 396 (1994).

[12] U. Fano, Phys. Rev. **124**, 1866 (1961).

[13] K. V. Klein, in *Light Scattering in Solids I*, edited by M. Cardona (Springer-Verlag, Heidelberg, 1983).

[14] R. J. McQueeney, Y. Petrov, T. Egami, M. Yethiraj, G. Shirane, and Y. Endoh, Phys. Rev. Lett. **82**, 628 (1999).